Quantum Electronics **49** (10) 901–904 (2019)

LASERS

https://doi.org/10.1070/QEL17050

Attainment of a 40 TW peak output power with a visible-range hybrid femtosecond laser system

S.V. Alekseev, N.G. Ivanov, V.F. Losev, G.A. Mesyats, L.D. Mikheev, N.A. Ratakhin, Yu.N. Panchenko

Abstract. **We report the results of investigations aimed at raising the peak output power of a THL-100 visible-range hybrid femtosecond laser system based on a XeF(C–A) photodissociation amplifier. The increase in power was achieved due to the shortening of the pulse duration at the system output by broadening the spectral profile of the second harmonic from 5.3 to 8 nm, which takes place in the transformation of a negatively chirped pulse of the fundamental frequency radiation in a nonlinear KDP crystal. After the KDP the radiation pulse was stretched to 1.8 ps in a prism stretcher and amplified in the XeF(C–A) amplifier. The energy obtained at the amplifier output was 1.2 J. After compression of the amplified output pulse, its duration was equal to 29.4 fs, which means that a peak output power of 40 TW was reached at the output of the laser system.**

Keywords: *hybrid laser system, XeF (C–A) photodissociation amplifier, Ti : sapphire front end, chirped pulse, stretcher, compressor.*

1. Introduction

At present, the development of ultrahigh-power laser systems with a pulse duration of 30–60 fs bases primarily on the application of solid-state Ti : sapphire or parametric amplifiers with the use of CPA technology [1]. Pulse stretching to a subnanosecond duration is required for decreasing the radiation power below the threshold one, whereby there occurs its self-focusing. After amplification, the pulse is compressed again to the initial duration in a compressor made of diffraction gratings. All these systems operate in the IR spectral range (0.8–1 μm). Expanding their spectral operating range permits the application domain of these systems to be enlarged and in many cases favours an increase in the efficiency of femtosecond radiation–matter interaction [2, 3]. The method of advancing to the visible spectral range by high harmonic generation of the fundamental IR radiation is well known. However, the possibility of converting ultrahigh-power IR radiation beams to the second harmonic (SH) is hindered by the technological problems of making thin (under 1 mm) nonlinear crystals of a sufficiently large diameter (20 cm and over). Furthermore, this method has one more significant drawback: the quality of the converted radiation with a femtosecond pulse duration is very low due to self-phase modulation, cross-phase modulation, Kerr self-focusing, and the deep modulation of the SH spectrum in the nonlinear crystal [4–7]. In this connection the 4-TW power achieved for the SH (λ = 400 nm; pulse duration τ = 60 fs) of Ti : sapphire radiation in 2005 [8] long remained a record for this method. It was not until 2017 that a peak radiation power of 270 TW (τ = 30 fs) was obtained for the SH (λ = 400 nm) on a high-power Ti:sapphire laser system [9]. The attainment of a power of 27 TW (τ = 60 fs) was reported in Ref. [10] in 2018, but a low quality of the SH beam was noted: in the beam focusing, only about 30% of the energy was contained in the diffraction-limited spot.

During the last decade, an alternative way of producing multiterawatt laser systems was developed at the Lebedev Physical Institute (LPI) (Moscow) and the Institute of High Current Electronics of the Siberian Branch of the Russian Academy of Sciences (IHCE SB RAS) (Tomsk). This way implies the use of a solid-state femtosecond laser complex and a XeF(C–A) photodissociation amplifier with a gaseous active medium [11–15]. The advantages of this hybrid system are low optical nonlinearity of the gaseous active medium, visible radiation range, possibility of scaling-up the gaseous amplifier, and attainment of a high contrast ratio due to the radiation conversion in a nonlinear crystal and to a low gain coefficient in the gaseous medium. In 2012, a peak output power of 14 TW was obtained with the THL-100 facility, which was record-high for the visible spectral range [13]. After that, the feasibility of raising this output power was studied in detail. To do this, several problems had to be solved, which were related to the SH beam nonuniformity arising in the radiation conversion in a nonlinear crystal, to the distortion-free beam passage through the prism stretcher and compressor, to the beam amplification in the gaseous amplifier without the development of Kerr self-focusing in the active medium, and, lastly, to the development of techniques for measuring the parameters of the radiation of multiterawatt power. These investigations, which were reported in our papers [16–26], resulted in obtaining an energy of 2.5 J in a pulse with τ = 2.35 ps and of 3.2 J in a pulse with τ = 50 ps [24, 25].

In the present paper we report the use of our previous results in the execution of experiments aimed at raising the peak output power of the THL-100 laser system. The increase in the output power became possible due to the shortening of the output pulse with retention of the beam uniformity throughout the optical path.

S.V. Alekseev, N.G. Ivanov, V.F. Losev, N.A. Ratakhin, Yu.N. Panchenko Institute of High Current Electronics, Siberian Branch, Russian Academy of Sciences, Akademicheskii prosp. 2/3, 634055 Tomsk, Russia; e-mail: losev@ogl.hcei.tsc.ru;
G.A. Mesyats, L.D. Mikheev Lebedev Physical Institute, Russian Academy of Sciences, Leninsky prosp. 53, 119991 Moscow, Russia

Received 25 April 2019; revision received 13 June 2019
Kvantovaya Elektronika **49** (10) 901–904 (2019)
Translated by E.N. Ragozin

2. Instrumentation and experimental technique

The THL-100 laser system comprises a Start-480M femtosecond Ti:sapphire front end made by Avesta-Project Ltd., a second harmonic generator, a prism stretcher, a XeF(C–A) photodissociation amplifier developed and made at the IHCE SB RAS, jointly with the LPI, and a compressor based on fused silica plates. The laser system is schematised in Fig. 1. The front end comprises a femtosecond Ti:sapphire master oscillator, a grating stretcher, a regenerative amplifier, two multipass amplifiers, and a grating pulse compressor. It operates at a pulse repetition rate of 10 Hz or in the single-pulse regime with external triggering. The front end provides a transform-limited 60–70 fs long output pulse at a centre wavelength of 950 nm with an energy of up to 50 mJ.

For a second harmonic generator we used a 1.8-mm-thick type-I KDP crystal. The prism stretcher consisted of fused silica prisms P1 and P2 and sweep mirrors. It stretched the femtosecond radiation pulse to a picosecond duration by negative group velocity dispersion. The picosecond pulse is amplified in the XeF(C–A) photodissociation amplifier in 33 passes through the active medium. To weaken the effect of diffraction of the amplified radiation at the mirror edges, a toothed aperture stop with an inner diameter of 13 mm and a tooth height-to-pitch ratio $h/d = 7$ was installed at the amplifier input. The amplifier was comprehensively described in our papers [13–15]. It is pumped by the VUV radiation of an electron-beam converter, which converts the energy of six electron beams to the UV radiation of xenon at $\lambda = 172$ nm. This radiation is introduced into a hexahedral 24-cm diameter cell through CaF_2 windows. The cell is filled with XeF_2 vapour with a partial pressure of 0.2–0.3 Torr and nitrogen to a pressure of 0.25–0.5 atm. The UV radiation results in the photodissociation of the XeF_2 vapour with the production of excited C state of XeF molecules. Stimulated emission arises in the transition of XeF molecules from state C to dissociative state A. A convex mirror M10 with a radius of curvature of –23 m is placed in front of the amplifier to geometrically match the beam diameter with the multipass mirror configuration of the amplifier. For the two last passages the beam was additionally expanded by the configuration's penultimate mirror with a radius of curvature of –5 m and then extracted from the cell in the form of a diverging (angle, 0.23 mrad) beam 12 cm in diameter. After that the beam was collimated with a spherical mirror M11 to a diameter of 20 cm and passed through a compressor consisting of three 4-cm-thick UV quartz plates arranged at the Brewster angle. The radiation energy loss in the compressor did not exceed 2%.

In these experiments the second harmonic was produced for a transform-limited and negatively chirped pulse of the fundamental frequency radiation. The chirp was provided by increasing the distance between the compressor gratings of the front end. The excess negative group velocity dispersion relative to a transform-limited pulse was equal to –23000 fs^2. To improve the conversion efficiency, prior to the KDP crystal the beam was compressed with a mirror telescope (mirrors M2, M3) to a diameter of 1 cm. The duration of the negatively chirped SH pulse was equal to 750 fs. After the KDP the second harmonic radiation was delivered to a prism stretcher, which lengthened the pulse to 1.8 ps, and was next amplified in the XeF(C–A) amplifier.

To measure the amplified pulse duration, the central part of the beam was focused with a spherical mirror M13 (diameter, 90 mm; focal length,12.2 m) and directed to an ASF-20-480 autocorrelator after reflection from the face of fused silica wedge W. An aperture stop 250 μm in diameter was placed at the focal waist in front of the autocorrelator. The light reflected from the second face of the wedge was used to record the spectral composition of the radiation with an HR4000CG-UV-NIR Ocean Optics spectrometer. Neutral light filters LF1 and LF2 were placed in front of the spectrometer in the amplification regime.

In the measurement of the amplified radiation energy, the diameter of the output XeF(C–A) amplifier beam was compressed to 4 cm with a Galilean telescope and directed to a fused silica wedge. The beam reflected from one face of the wedge was recorded with a Gentec energy meter. The real energy was calculated by taking into account the reflection

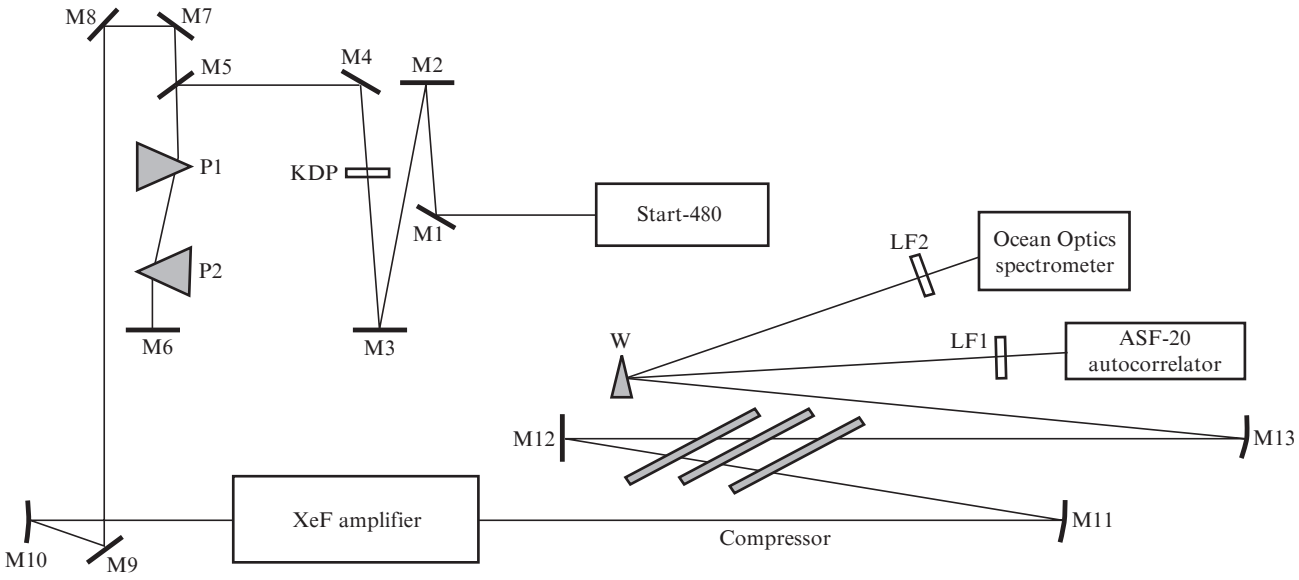

Figure 1. Schematic of the laser system:(M1, M4–M9, M12) plane folding mirrors; (M2, M3) telescope mirrors; (P1, P2) stretcher prisms; (M10) convex mirror of radius 23 m; (M11) concave mirror of radius 15 m; (M13) concave mirror of radius 24.4 m; (W) wedge; (LF1, LF2) light filters.

coefficients of the wedge face and the lens surfaces of the Galilean telescope. Behind the wedge we placed photographic paper for recording the spatial distribution of laser radiation intensity, which was processed using the Beam code.

3. Results and their discussion

When planning these experiments, we analysed the conditions for the laser beam passage through the elements of the optical configuration and the active medium in order to rule out nonlinear effects in them. This analysis suggests that these conditions will be fulfilled when the output energy of the laser system does not exceed 1.5 J. In order for this to take place, the output pulse energy of the front end should be equal to about 0.1 mJ, the nitrogen pressure in the laser cell be equal to 0.25 atm, and the XeF_2 vapour pressure to 0.2 Torr. The conversion of the chirped pulse at the fundamental frequency in the KDP made it possible to broaden the spectral profile and shorten the duration of the transform-limited SH pulse after the compressor.

Figure 2a shows the spectra of the transform-limited and chirped pulses of the SH after the KDP. One can see that the halfwidth of the chirped pulse spectrum increased from 5.3 to 8 nm. Furthermore, its spectral profile exhibits intensity modulations. The pulse chirping made it possible to eliminate Kerr self-focusing in the nonlinear crystal [22] and to lower the beam distortions in the stretcher prisms [17]. The radiation spectrum broadening permitted shortening the thickness of the quartz glass in the compressor for a negatively chirped pulse duration of 1.8 ps. According to our estimates, this is the shortest duration that rules out the nonlinearities in the active medium of the gas amplifier. A spectrum width of 5.3 nm and a chirped pulse duration of 1.8 ps would have required an approximately 1.5 times greater quartz thickness in the compressor.

Prior to the execution of experiments involving beam amplification in the XeF(C–A) amplifier, we measured the radiation pulse duration and the pulse spectrum at the amplifier output in the absence of pumping. The recorded duration of the transform-limited SH pulse was equal to ~30 fs and its spectrum was hardly different from the radiation spectrum after the KDP crystal.

Then we performed experiments to amplify negatively chirped pulses in the XeF(C–A) amplifier. In this case, the radiation energy at its input was equal to 70 μJ. The amplified pulse energy was equal to 1–1.2 J. The shape and spatial intensity distribution of the amplified beam is depicted in Fig. 3. One can see that the output radiation intensity distribution is close to a super-Gaussian one. Figure 2b shows the amplified radiation spectrum, whose width remains at a level of 8 nm after amplification but the spectral profile is some-

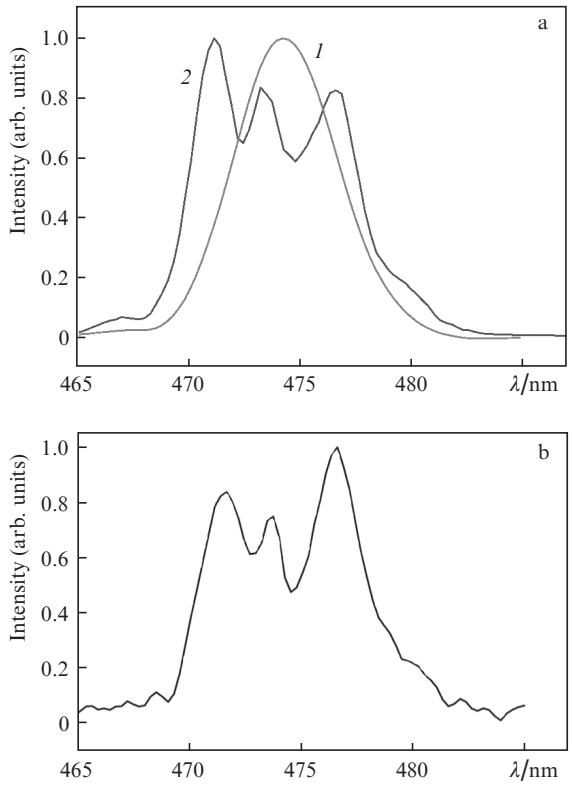

Figure 2. Spectra (a) of (*1*) transform-limited and (*2*) chirped SH radiation pulses prior to amplification in the gas amplifier and (b) of the amplified radiation at the output of the laser system after compressor.

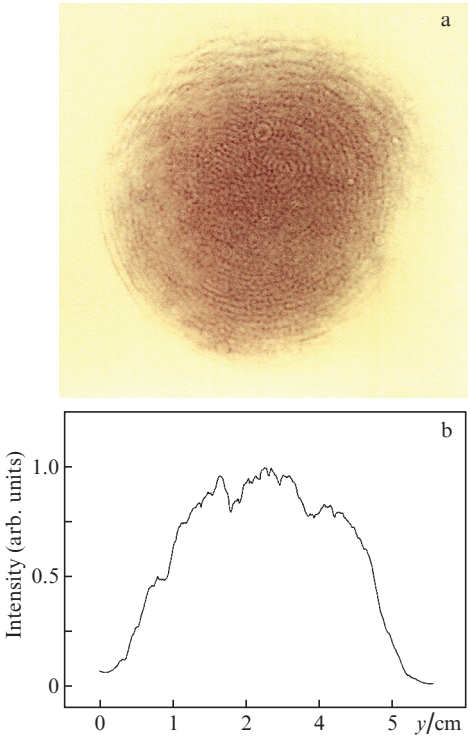

Figure 3. (a) Autograph and (b) spatial intensity distribution of the beam amplified in the XeF(C–A) amplifier.

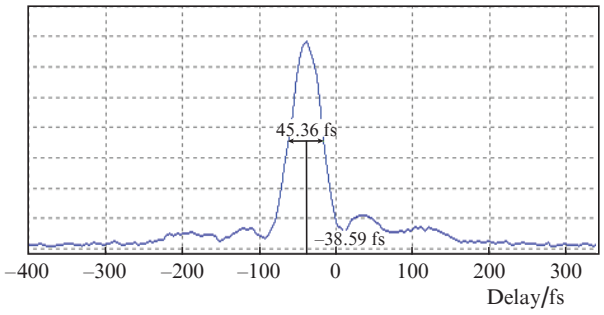

Figure 4. Autocorrelation function of the amplified radiation pulse of duration 29.4 ± 1.4 fs.

what changed due to an increase in long-wavelength component intensities. This is attributable to the fact that the amplification profile peaks near 481 nm [27]. Measurements of the amplified pulse duration with an autocorrelator in the $sech^2$ approximation yielded a figure of 29.4 fs (Fig. 4). The resultant data suggest, with account of the loss in the compressor (2%), that a peak output laser power of 40 TW was obtained. To date, as far as we know, this result ranks second in the peak radiation power for the visible spectral region.

4. Conclusions

Therefore, we report an increase in the peak output pulse power of the THL-100 hybrid laser system, which operates in the visible spectral region (475 nm), from 14 to 40 TW. It has been possible to raise the output power by broadening the spectrum at the output of the front end and improving the amplified beam quality. The spectral profile of the SH was broadened from 5.3 to 8 nm in a nonlinear crystal by chirping the output pulse of the fundamental frequency with the use of the compressor of the front end. Increasing the fundamental-harmonic pulse duration to 750 fs during chirping made it possible to rule out the Kerr self-focusing in the nonlinear crystal and to transmit the longer SH pulse without distortions through a prism stretcher, in which its duration lengthened to 1.8 ps. The broadening of the radiation spectrum permitted the quartz glass thickness in the compressor at the output of the system to be decreased in comparison with the case of a 50-fs long pulse, and the shortening of the output pulse permitted the output power to be increased for a moderate energy. These all are important factors making it possible to decrease the nonlinear phase incursion in the compressor. By amplifying the negatively chirped pulse in the XeF(C–A) amplifier, an energy of 1.2 J was obtained. Passing the pulse through the compressor made of fused quartz plates shortened its duration to 29.4 fs.

Acknowledgements. Experiments in the spectrum broadening and compression of the output pulse of the front end were supported by the Russian Science Foundation (Grant No. 18-19-00009). Experiments in the amplification of the 1.8-ps long radiation pulse in the XeF(C–A) amplifier were supported by the Russian Foundation for Basic Research (Grant No. 18-08-00383a).

References

1. Strickland D., Mourou G.A. *Opt. Commun.*, **56**, 219 (1985).
2. Mikheev L.D., Tcheremiskine V.I., Uteza O.P., Sentis M.L. *Progr. Quantum Electron.*, **36**, 98 (2012).
3. Mikheev L.D., Losev V.F., in *High Energy and Short Pulse Lasers* (Croatia: InTech, 2016) Ch. 6, pp 131–161.
4. Begishev I.A., Kalashnikov M., Karpov V., et al. *J. Opt. Soc. Am.*, **21**, 318 (2004).
5. Ginzburg V.N., Lozhkarev V.V., Mironov S.Yu., et al. *Quantum Electron.*, **40**, 503 (2010) [*Kvantovaya Elektron.*, **40**, 503 (2010)].
6. Mironov S.Yu., Ginzburg V.N., Lozhkarev V.V., et al. *Quantum Electron.*, **41**, 963 (2011) [*Kvantovaya Elektron.*, **41**, 963 (2011)].
7. Horlein R., Dromey B., Adams D., et al. *New J. Phys.*, **10**, 083002 (2008).
8. Toth R., Kieffer J.C., Fourmaux S., Ozaki T. *Rev. Sci. Instrum.*, **76**, 083701 (2005).
9. Yong Wang, Shoujun Wang, Alex Rockwood, et al. *Opt. Lett.*, **42**, 3828 (2017).
10. Curtis A., Calvi C., Tinsley J., et al. *Nat. Commun.*, **9**, 1077 (2018).
11. Mikheev L.D. *Laser Part. Beams*, **10**, 473 (1992).
12. Aristov A.I., Grudtsyn Ya.V., Zubarev I.G., et al. *Opt. Atmos. Okeana*, **22**, 1029 (2009).
13. Alekseev S.V., Aristov A.I., Ivanov N.G., et al. *Quantum Electron.*, **42**, 377 (2012) [*Kvantovaya Elektron.*, **42**, 377 (2012)].
14. Alekseev S.V., Aristov A.I., Ivanov N.G., et al. *Laser Part. Beams*, **31**, 17 (2013).
15. Alekseev S.V., Aristov A.I., Grudtsyn Ya.V., et al. *Quantum Electron.*, **43**, 190 (2013) [*Kvantovaya Elektron.*, **43**, 190 (2013)].
16. Alekseev S.V., Ivanov N.G., Ivanov M.V., Losev V.F., Panchenko Yu.N. *Izv. Ross. Akad. Nauk, Ser. Fiz.*, **79**, 266 (2015).
17. Ivanov M.V., Alekseev S.V., Ivanov N.G., Losev V.F. *Proc. SPIE*, **9810**, 98100J (2015).
18. Alekseev S.V., Ivanov N.G., Losev V.F., Mironov S.Yu. *Opt. Atmos. Okeana*, **29**, 243 (2016).
19. Ivanov N.G., Ivanov M.V., Losev V.F., Yastremskii A.G. *Izv. Vyssh. Uchebn. Zaved., Ser. Fiz.*, **59**, 65 (2016).
20. Yastremskii A.G., Ivanov N.G., Losev V.F. *Quantum Electron.*, **46**, 982 (2016) [*Kvantovaya Elektron.*, **46**, 982 (2016)].
21. Ivanov N.G., Losev V.F. *Izv. Vyssh. Uchebn. Zaved., Ser. Fiz.*, **61**, 76 (2018).
22. Alekseev S.V., Ivanov M.V., Ivanov N.G., Losev V.F. *Izv. Ross. Akad. Nauk, Ser. Fiz.*, **83**, 320 (2019).
23. Losev V.F., Alekseev S.V., Ivanov M.V., et al. *Proc. SPIE*, **11042**, 110420P (2019).
24. Alekseev S.V., Ivanov N.G., Ivanov M.V., et al. *Quantum Electron.*, **47**, 184 (2017) [*Kvantovaya Elektron.*, **47**, 184 (2017)].
25. Alekseev S.V., Ivanov N.G., Ivanov M.V., et al. *Izv. Vyssh. Uchebn. Zaved., Ser. Fiz.*, **59**, 75 (2017).
26. Ivanov N.G., Losev V.F. *Opt. Atmos. Okeana*, **29**, 133 (2016).
27. Bischek W.K., Ecstrom D.J., Walfer H.C., Tilton R.A. *J. Appl. Phys.*, **52**, 4429 (1981).